Structure–activity relationships of galabioside derivatives as inhibitors of *E. coli* and *S. suis* adhesins: nanomolar inhibitors of *S. suis* adhesins†

Jörgen Ohlsson,[a] Andreas Larsson,[b] Sauli Haataja,[c] Jenny Alajääski,[c] Peter Stenlund,[d] Jerome S. Pinkner,[e] Scott J. Hultgren,[e] Jukka Finne,*[c] Jan Kihlberg*[b] and Ulf J. Nilsson*[a]

[a] *Organic Chemistry, Lund University, P.O. Box 124, SE-221 00 Lund, Sweden.*
E-mail: ulf.nilsson@organic.lu.se; Fax: (+46) 46 222 82 09; Tel: (+46) 46 222 82 18

[b] *Organic Chemistry, Department of Chemistry, Umeå University, SE-901 87 Umeå, Sweden*

[c] *Department of Medical Biochemistry and Molecular Biology, University of Turku, FI-20520 Turku, Finland*

[d] *Biochemistry, Department of Chemistry, Umeå Universitet, SE-901 87 Umeå, Sweden*

[e] *Department of Molecular Biology, Washington University School of Medicine, St. Louis, Missouri 63110, USA*

Four collections of Galα1-4Gal derivatives were synthesised and evaluated as inhibitors of the PapG class II adhesin of uropathogenic *Escherichia coli* and of the P_N and P_O adhesins of *Streptococcus suis* strains. Galabiosides carrying aromatic structures at C1, methoxyphenyl *O*-galabiosides in particular, were identified as potent inhibitors of the PapG adhesin. Phenylurea derivatisation at C3′ and methoxymethylation at O2′ of galabiose provided inhibitors of the *S. suis* strains type P_N adhesin with remarkably high affinities (30 and 50 nM, respectively). In addition, quantitative structure–activity relationship models for *E. coli* PapG adhesin and *S. suis* adhesin type P_O were developed using multivariate data analysis. The inhibitory lead structures constitute an advancement towards high-affinity inhibitors as potential anti-adhesion therapeutic agents targeting bacterial infections.

Introduction

The alarming increase in the resistance of bacteria to traditional antibiotics[1–3] makes it imperative to develop alternative ways of treating bacterial infections. The majority of infectious diseases are initiated by adhesion of pathogenic organisms to host tissue and in many cases glycoconjugates present on the mammalian cell surface, *e.g.* glycoproteins and glycolipids, act as receptors for a wide variety of extracellular bacterial proteins termed adhesins.[4,5] This carbohydrate–protein interaction is often a pre-requisite for the later stages of bacterial infection and inhibitors of this recognition process are potential pharmaceutical agents. Bacterial resistance towards such anti-adhesive drugs is believed to evolve slowly because the infecting bacteria are not killed and are consequently not under selection pressure.

Two well-known examples of pathogenic bacteria adhering to glycoconjugates are uropathogenic *Escherichia coli*, which is the main cause of urinary tract infections, and *Streptococcus suis*, which causes meningitis in pig and man. The majority of *E. coli* bacteria causing pyelonephritis (kidney infection) adhere *via* proteinaceous appendices, termed P-pili. These pili are terminated with an adhesin, PapG, that binds to the Galα1-4Gal (galabiose)[6–8] moiety present in the globoseries of glycolipids on uroepithelial cells and erythrocytes. Three different classes of the PapG adhesin (classes I–III)[9,10] have been identified based on different erythrocyte agglutination patterns. Pyelonephritis in both children and adult women is associated with PapG class II,[11,12] while class III is associated with cystitis in adult women.[13] In addition to anchoring the bacteria to the host cell, the adhesion of PapG induces the release of ceramides[14] that are important second messenger molecules, and results in up-regulation of, and eventual secretion of, several immunoregulatory cytokines from host cells.[15] *Streptococcus suis* is a frequent

colonizer of the pig respiratory tract. Galα1-4Gal terminating oligosaccharides have been shown to be optimal receptors for *S. suis*. Systematic competitive inhibition studies characterized the key hydroxyl groups that are required for binding to Galα1-4Gal and also classified the adhesion activities into two types, P_N and P_O.[16]

Most natural carbohydrate ligands bind lectins with low affinity (K_d normally in the 0.1–1 mM range). One attractive strategy to overcome this problem is to use a small key saccharide as the core structure and attach substituents that interact with the lectin in a favourable manner. It has been shown that for the PapG class II adhesin the galabiose disaccharide is such a key structure[17] necessary for recognition and that galabioside derivatives substituted at C1 and C3′ often display enhanced affinity for the PapG adhesins.[18] Furthermore, the crystal structure of the class II PapG adhesin in complex with the globotetraose tetrasaccharide has been solved[19] and it confirmed that the galabiose disaccharide unit is the most critical structural element for the formation of the complex. The complex structure revealed an extended surface composed of H1, H2 and H6 of Galα, H1, H3, H4, H5 and H6 of Galβ, and H2 and H4 of Glc, that make hydrophobic contact primarily with the Trp107 sidechain. The adhesin additionally forms four hydrogen bonds to HO4, O5 and HO6 of the non-reducing GalNAc residue, seven to HO2, O3, HO4 and HO6 of the Galα residue, four to HO3, O5 and HO6 of the Galβ, and three to HO2 and HO3 of the Glc residue. Apparently, the two residues flanking galabiose, GalNAc and Glc, are involved *via* hydrophobic contacts and hydrogen bonding (*e.g.* Lys172 to GalNAc and Arg170 and Trp107 to Glc), but to a lesser extent.

The galabiose disaccharide has also been shown to be the key recognition element for adhesins from *S. suis* strains of both type P_N and P_O. The two adhesins from *S. suis*, however, display differences in the sub-molecular details of galabiose recognition.[16] Multivalent galabiose derivatives have been reported to display greatly enhanced affinity.[20] However, although

---

† Jörgen Ohlsson, Andreas Larsson and Sauli Haataja contributed equally.

multivalent galabiosides provide potent inhibitors, they all share the disadvantages of large size and high polarity resulting in poor bioavailability.

The present paper describes an attempt to improve the affinity of inhibitors for the PapG class II adhesins and the two *S. suis* adhesins by the synthesis of four collections of galabiosides modified at C1 and C3′ in four different ways. In order to position the substituents at C1 as close as possible to the galabiose core structure, either amide formation (galabioside collection I), glycosylation of alcohols (collection II), or of thiols (collection III) were employed. At C3′, amide formation was used to create structural diversity on a *p*-methoxyphenyl galabioside core structure (collection IV). Recently reported synthesis and evaluation of earlier generations of galabiose derivatives has shown that the *p*-methoxyphenyl galabioside itself is an excellent inhibitor of the PapG adhesins.[18,21] The further evaluation of these earlier generations of galabiose derivatives against the two *S. suis* adhesins is also reported herein. In addition, quantitative structure–activity relationship models for *E. coli* PapG adhesin and *S. suis* adhesin type P_O were developed using multivariate data analysis.

Results and discussion

Synthesis of galabiose collections I–IV (Table 1)

For the synthesis of the collection I galabiosides, the galabiosyl bromide 1[22] was converted to the β-azide 4 (Scheme 1) *via* treatment with trimethylsilyl azide and tetrabutylammonium fluoride,[23] (3, 92%) followed by conventional deacylation with methanolic sodium methoxide to give 4 in 96% yield.
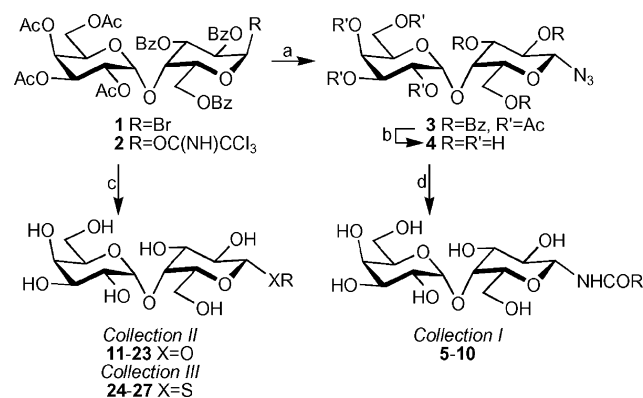
*Scheme 1* a) TMSN₃, Bu₄NF, THF, 92%. b) NaOMe, MeOH, 96%. For c) and d) see Table 1.

Hydrogenation of 4 over Pd/C in methanol gave an intermediate amine, which was immediately converted to amides by treatment with five different acid chlorides in the presence of sodium carbonate in THF, affording compounds 5–9 in 48–90% overall yields and β/α ratios of ~15 : 1. No product was observed under these reaction conditions with a hindered acid chloride (*i.e.* 10). However, acylation with the acid chloride, pyridine, and a catalytic amount of DMAP, gave compound 10 in a moderate 28% yield. Attempts to increase the yields for compounds 6–9 with these latter reaction conditions were unsuccessful. Furthermore, different reaction conditions were unsuccessfully evaluated in attempts to improve the β-selectivities (*i.e.* PtO₂ as a hydrogenation catalyst, one-pot azide reduction and acylation, hydrogenation in the presence of HCl, and the use of different solvents). It is likely that the anomerisation of the amine occurs faster than the acylation, because similar α/β ratios were obtained under all conditions tried. No α-anomer was detected when fully acylated lactosyl azide[24] was reacted under the same reaction conditions, suggesting that the resulting anomeric mixtures obtained in the case of the galabiose derivatives 5–10

are probably due to the inherent properties of galactose (or galabiose).

Collection II galabiose derivatives were prepared from either the galabiosyl α-trichloroacetimidate 2 (compounds 11–18) or from the galabiosyl bromide 1 (compounds 19–22). Trimethylsilyl trifluoromethanesulfonate (TMSOTf)-promoted glycosylation of aromatic and aliphatic alcohols with the trichloroacetimidate 2, followed by deacylation in methanolic sodium methoxide, furnished compounds 11–18 in 44–83% yield (β/α ~15 : 1). Under these conditions, phenols carrying electron withdrawing groups typically gave low yields and poor α/β-selectivities. Instead, nucleophilic displacement of the galabiosyl bromide 1 with the corresponding sodium phenolates fortunately afforded compounds 19–22 in 36–70% yield after deacylation. Complete β-selectivity was observed for compounds 20–22, while compound 19 had a β/α-ratio of about 10 : 1. Compound 23 was prepared from 22 by catalytic hydrogenation followed by acylation under conditions similar to those described for the preparation of collection I.

Galabioside collection III was prepared by nucleophilic displacement of the galabiosyl bromide 1 with thiophenolates, followed by deacylation, to furnish β-galabiosides 24–27 in 76–88% yield.

Synthesis of collection IV required the introduction of a handle (amine) at C3′ of *p*-methoxyphenyl galabioside (Scheme 2). Henceforth, the known galactoside 28[25] was deacylated and benzylated to give the galactosyl donor 29. α-Galactosylation of the acceptor 30,[22] using *N*-iodosuccinimide-trimethylsilyl trifluoromethanesulfonate as promoter,[26,27] gave the protected 3′-azido galabioside 31 in 93% yield. Debenzoylation in methanolic sodium methoxide gave 32 in 80% yield, the key starting material for the synthesis of galabioside collection IV.
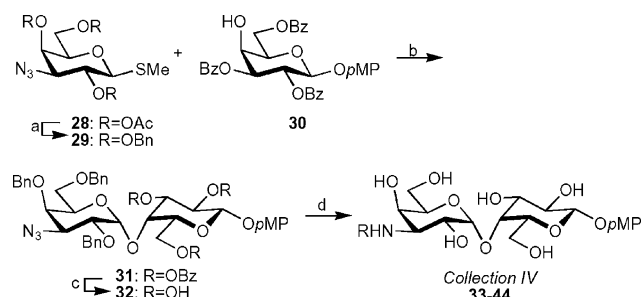
Scheme 2 a) iNaOMe, MeOH, iiNaH, BnBr, DMF, 86%. b) NIS, TMSOTf, CH₂Cl₂–Et₂O (1 : 2), −50 °C, 93%. c) NaOMe, MeOH, 80%. d) See Table 1.

The azido group of galabioside 32 was reduced to the amine 33 under reaction conditions similar to those described for the preparation of collection I, with the exception that 2 equivalents of HCl were added to ensure complete hydrogenolysis of the benzyl groups. The 3′-amino galabioside 33 was treated with sodium carbonate and either an acyl chloride (34–35 and 37–41), acid anhydride (36 and 42), or isocyanate (43–44) to give galabiosides 34–44 in 49–83% yield.

Binding of the *E. coli* PapG class II adhesin to galabioside derivative collections I–IV

Binding of galabiose derivative collections I–IV by an *N*-terminal 196 amino acid truncate of the class II PapG adhesin[19] was determined by surface plasmon resonance as recently described.[21] The binding data were analysed using the software Scrubber[28] (Fig. 1, Table 1).

The presence of amides at C1 of galabiose (collection I) turned out to be detrimental to binding. The benzamido derivatives (5–8, and 10) displayed K_d of 1.0–2.3 mM, which is much worse than that of the known reference compound *p*-methoxyphenyl galabioside 45[18] (K_d 140 μM[21]). Virtually no interaction was seen with an aliphatic amide at C1 (9). The amide-functionality at

Table 1 Synthesis and biological evaluation of galabiose collections I–IV (**4–44**) and the known galabiosides **45–64**. Dissociation constants for binding to the class II PapG adhesin were determined by surface plasmon resonance, whereas IC_{50} values for the P_N and P_O adhesins from *S. suis* strains were determined by hemagglutination inhibition
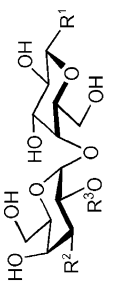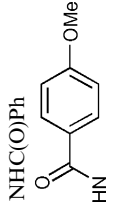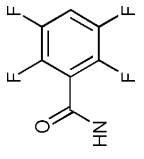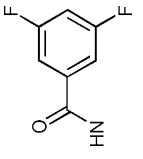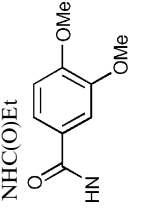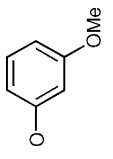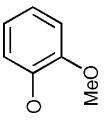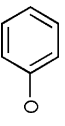

Compound/conditions[a]/yield (%)	R^1	R^2	R^3	K_d/μM *E. coli* PapG II	IC_{50}/μM *S. suis* P_N/P_O
Collection I					
5/A/90	NHC(O)Ph (4-OMe benzamide)	OH	H	2340	7.8/5.0
6/A/61		OH	H	1030	2.5/2.5
7/A/51	(tetrafluoro benzamide)	OH	H	1640	2.5/2.5
8/A/54	(3,5-difluoro benzamide)	OH	H	1190	2.5/2.5
9/A/48	NHC(O)Et (3,4-dimethoxy benzamide)	OH	H	3030	2.5/1.25
10/B/28		OH	H	1320	0.98/7.8
Collection II					
11/C/53	(3-OMe phenoxy)	OH	H	150	2.5/1.25
12/C/74	(2-OMe phenoxy)	OH	H	176	7.8/5.0
13/C/66	(phenoxy)	OH	H	170	0.63/0.31

Table 1 *(Contd.)*
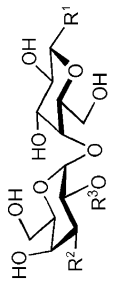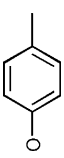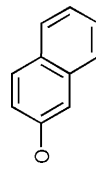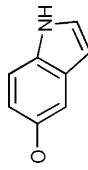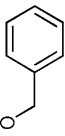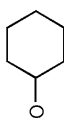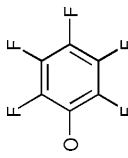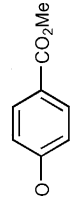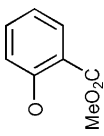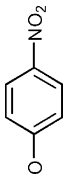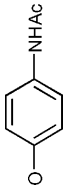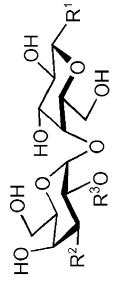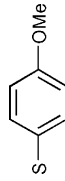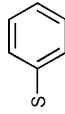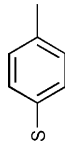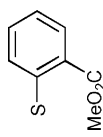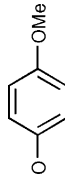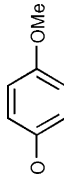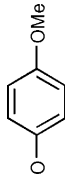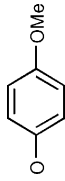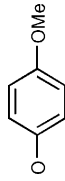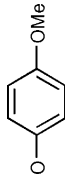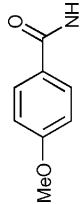
Compound/conditions[a]/yield (%)	R^1	R^2	R^3	$K_d/\mu M$ *E. coli* PapG II	$IC_{50}/\mu M$ *S. suis* P_N/P_O
14/C/80	(4-methylphenyl)-O	OH	H	191	0.63/0.63
15/C/62	(naphthalen-2-yl)-O	OH	H	217	0.31/0.63
16/C/44	(1H-indol-5-yl)-O	OH	H	217	0.63/0.63
17/C/78	(benzyl)-O	OH	H	512	0.63/0.63
18/C/83	(cyclohexyl)-O	OH	H	269	0.63/0.63
19/C/65	(pentafluorophenyl)-O	OH	H	373	0.63/0.31
20/D/54	(4-CO_2Me-phenyl)-O	OH	H	229	0.63/0.63
21/D/36	(2-MeO_2C-phenyl)-O	OH	H	235	7.8/2.5
22/D/70	(4-NO_2-phenyl)-O	OH	H	189	0.63/0.63
23/E/68	(4-NHAc-phenyl)-O	OH	H	180	0.63/0.31

Table 1 *(Contd.)*

Compound/conditions[a]/yield (%)	R^1	R^2	R^3	K_d/μM *E. coli* PapG II	IC$_{50}$/μM *S. suis* P$_N$/P$_O$
Collection III					
24/E/76	S–C$_6$H$_4$–OMe	OH	H	605	0.63/0.31
25/E/79	S–C$_6$H$_5$	OH	H	321	0.63/0.31
26/E/85	S–C$_6$H$_4$–CH$_3$	OH	H	428	5.0/0.31
27/E/88	S–C$_6$H$_4$–CO$_2$Me	OH	H	333	2.5/1.25
Collection IV					
33/F/93	O–C$_6$H$_4$–OMe	NH$_2$	H	4110	15.6/2.5
34/G/74	O–C$_6$H$_4$–OMe	CH$_3$C(O)NH	H	23500	0.63/15.6
35/G/79	O–C$_6$H$_4$–OMe	CH$_3$CH$_2$C(O)NH	H	30500	1.25/62.5
36/G/78	O–C$_6$H$_4$–OMe	HO$_2$C(CH$_2$)$_2$C(O)NH	H	500000	0.63/31.3
37/G/70	O–C$_6$H$_4$–OMe	PHC(O)NH	H	34500	0.63/62.2
38/G/66	O–C$_6$H$_4$–OMe	MeO–C$_6$H$_4$–C(O)NH	H	14000	0.63/31.3

Table 1 *(Contd.)*
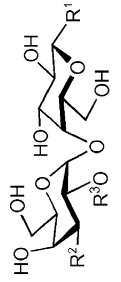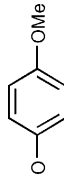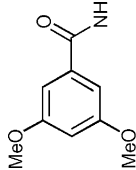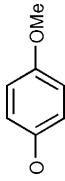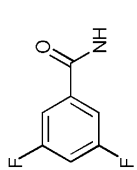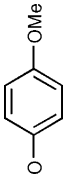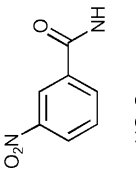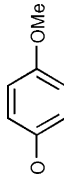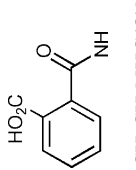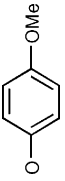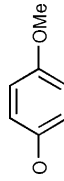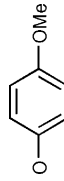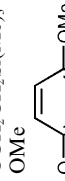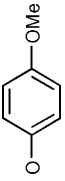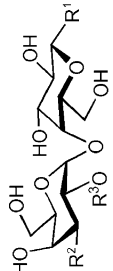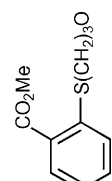
Compound/conditions[a]/yield (%)	R^1	R^2	R^3	K_d/µM *E. coli* PapG II	IC$_{50}$/µM *S. suis* P$_N$/P$_O$
39/G/61	(4-OMe-phenyl)-O	MeO—benzamide—NH (3,5-diOMe)	H	99000	0.31/31.3
40/G/83	(4-OMe-phenyl)-O	F—benzamide—NH (3,5-diF)	H	11400	1.25/62.5
41/G/69	(4-OMe-phenyl)-O	O$_2$N—benzamide—NH	H	76700	0.63/62.5
42/G/55	(4-OMe-phenyl)-O	HO$_2$C—benzamide—NH	H	141000	1.25/62.5
43/G/49	(4-OMe-phenyl)-O	CH$_3$CH$_2$NHC(O)NH	H	10100	0.31/62.5
44/G/84	(4-OMe-phenyl)-O	PhNHC(O)NH	H	27200	0.04/62.5
Known galabioside					
45	(4-OMe-phenyl)-O	OH	H	140[21]	0.31/0.31
46	OCH$_2$CH$_2$Si(Me)$_3$	OH	H	646[21]	0.63/0.63
47	OMe	OH	H	306[21]	0.63/0.63
48	(4-OMe-phenyl)-O	OH	Me	150[21]	0.63/3.9
49[35]	NHC(O)Ph	OH	Me	n.d.	5.0/31.3

Table 1 *(Contd.)*

Compound/conditions[a]/yield (%)	R¹	R²	R³	K_d/μM *E. coli* PapG II	IC₅₀/μM *S. suis* P_N/P_O
50	(4-OMe-phenyl)O	OH	Pr	1000[21]	0.31/5.0
51	(4-OMe-phenyl)O	OH	MeOCH₂	490[21]	0.08/15.6
52[18]	(4-OMe-phenyl)O	PhCH₂O	H	n.d.	2.5/1.25
53	(4-OMe-phenyl)O	CH₂=CHCH₂O	H	199[21]	2.5/3.9
54	(4-OMe-phenyl)O	(3-O₂N-benzyl)CH₂O	H	175[21]	2.5/1.25
55[18]	(4-OMe-phenyl)O	HO₂CCH₂O	H	n.d.	1.25/5.0
56[18]	(4-OMe-phenyl)O	MeO₂CCH₂O	H	n.d.	7.8/31.3
57[18]	(4-HO-phenyl)O(CH₂)₂S	cyclohexyl-S(CH₂)₃O	H	n.d.	15.6/15.6
58[18]	(2-MeO₂C-phenyl)O(CH₂)₂S	cyclohexyl-S(CH₂)₃O	H	n.d.	15.6/31.3
59[18] **60**[18]	OEt / (4-HO-phenyl)O(CH₂)₂S	PrO, NHAc, MeO₂C, S(CH₂)₃O	H / H	n.d. / n.d.	0.63/15.6 / 1.25/15.6
61[18]	(4-HO-phenyl)O(CH₂)₂S	HO(CH₂)₂S(CH₂)₃O	H	n.d.	7.8/7.8

Table 1 (*Contd.*)

Compound/conditions[a]/yield (%)	R¹	R²	R³	K_d/μM *E. coli* PapG II	IC$_{50}$/μM *S. suis* P_N/P_O
62[18]	O(CH₂)₂S–CH(CO₂Me)CH₂–NHAc	benzene ring with CO₂Me and S(CH₂)₃O	H	n.d.	5.0/2.5
63[18]	O(CH₂)₂S–CH(CO₂Me)CH₂–NHAc	MeO₂CCH₂S(CH₂)₃O	H	n.d.	5.0/31.3
64[18]	O(CH₂)₂S–CH(CO₂Me)CH₂–NHAc	NHAc, S(CH₂)₃O, MeO₂C	H	n.d.	5.0/31.3

[a] A) [i]4, H₂ (1 atm), Pd/C (10%), MeOH. [ii]RC(O)Cl, Na₂CO₃, THF. B) [i]4, H₂ (1 atm), Pd/C (10%), MeOH. [ii]RC(O)Cl, DMAP, pyridine. C) [i]10, R′-OH, TMSOTf, CH₂Cl₂, [ii]NaOMe, MeOH. D) [i]1, NaH, R′-OH, DMF, [ii]NaOMe, MeOH. E) [i]1, NaH, R-SH, DMF, [ii]1, NaOMe, MeOH. [iii]Ac₂O, Na₂CO₃, THF. E) [i]22, H₂ (1 atm), Pd/C (10%), MeOH, [ii]RC(O)Cl, RC(O)OR, or RNCO, Na₂CO₃, THF. F) 32, H₂ (1 atm), HCl (aq), Pd/C (10%), MeOH. G) 33, RC(O)Cl, RC(O)OR, or RNCO, Na₂CO₃, THF.

Fig. 1 Equilibrium isotherms fit to a 1 : 1 interaction model for **45** (△), **25** (■), **46** (□) and **36** (○) binding to PapGII immobilized to a CM5 surface plasmon resonance biosensor surface. The binding responses at equilibrium were normalised against maximum binding (*R*max). In cases where the affinity of the galabioside was too low (**36**) to saturate an expected binding isotherm, the *R*max was determined using a reference substance and the galabioside's molecular weight.

C1 probably positions the aromatic rings of **5–8** and **10** in non-favourable positions relative to the side chains of Trp107 and Arg170 of PapGII. In contrast, the *p*-methoxyphenyl glycoside of galabiose **45** positions the aromatic ring to interact favourably with Trp107 and Arg170, resulting in a K_d as low as 140 μM.[21]

Collection II (*O*-galabiosides **11–23**) turned out to be more successful in providing ligands for the class II PapG adhesin. All compounds showed higher affinities for the adhesin than those observed for aliphatic galabiosides (*i.e.* the 2-(trimethylsilyl)ethyl galabioside **46**[18]). The positions of methoxy groups on the aromatic aglycons had some impact on the affinity. *p*-Methoxyphenyl galabioside **45** and *m*-methoxyphenyl galabioside **11** had virtually the same K_d. However, the K_d (176 μM) for *o*-methoxyphenyl galabioside **12** was somewhat higher than **45** and close to that of the phenyl galabioside **13** (170 μM). Thus, the methoxyphenyl group interacts favourably with the adhesin when positioned in the *m*- or *p*-position. Exchange of the *p*-methoxy for a *p*-methyl group (*i.e.* **14**) resulted in an increase in K_d in the same range as removal of the *p*-methoxy group did. This suggests that the oxygen atom of the *p*-methoxy group is important for affinity to the adhesin. Introduction of other groups at the *p*-position of a phenyl aglycon (*i.e.* methylester **20**, nitro **22**, or acetamido **23**) resulted in galabiosides with the same K_d as the *p*-methylphenyl galabioside **14**, as did introduction of a methylester at the *o*-position (**21**). In contrast, the introduction of fluorine (**19**) resulted in a large increase in K_d to 373 μM, *i.e.* 2.5 times of that observed for phenyl galabioside **13**. Increasing the size of the aromatic substituent (*i.e.* naphthyl **15** or indolyl **16**) or moving the aromatic substituent away from the galabiose C1 (*i.e.* benzyl galabioside **17**), resulted in lowered affinity for the adhesin compared to phenyl galabioside **13**, further demonstrating the sensitivity towards the exact position of the aromatic substituents at C1. Furthermore, cyclohexyl galabioside **18** (K_d 269 μM) was a less potent inhibitor than phenyl galabioside **13**, suggesting that aromatic aglycons are beneficial. Most likely, phenyl aglycons of galabiosides stabilise complex formation *via* interactions with the aromatic side chain of Trp107 and with the guanidino group of Arg170 in the PapGII adhesin.[21]

Exchange of the anomeric oxygen atom for sulfur results in more hydrolytically stable galabiosides. However, the phenyl thio-galabiosides **24–27** (collection III) had K_d values in the 320–600 μM range, *i.e.* about one third of the affinity of their *O*-glycosidic counterparts. An altered conformation of phenyl thio-galabiosides, compared to the corresponding *O*-glycosides,[29] most likely explains the higher K_d values observed for these compounds. The aromatic aglycons of **24–26** are folded

back onto the galabiose disaccharide moiety, which causes a conformational change in the α(1–4) disaccharide linkage of galabiose. Hence, the phenyl thio-galabiosides **24–26** must adopt a high-energy conformation in order to be recognised by the class II PapG adhesin.

Exchange of a hydroxyl for an amino group at C3′ (**33**) turned out to be detrimental for binding; the K_d value for **33** was 29 times higher than that of *p*-methoxyphenyl galabioside **45**. Functionalisation of the amine at C3′ (**34–44**) resulted in even worse inhibitors (K_d 10–500 mM). The reason for the low affinity could be that the interaction between the Lys172 and O3′ seen in the crystal structure between the adhesin and the Gb4 tetrasaccharide is lost when an amine, amide or urea replaces the hydroxyl at C3′ of the galabiose disaccharide.

Binding of the *S. suis* adhesins type P_N and type P_O to galabioside derivative collections I–IV (5–44) and to known galabioside derivatives 45–64

Binding of galabiose derivatives **5–64** by *S. suis* types P_N and P_O was determined by hemagglutination inhibition essentially as previously described.[30] The galabiose substituents of **5–64** clearly interact with the two *S. suis* adhesins as the structures of the substituents exert large influences on their inhibitory powers (Table 1). Furthermore, the two adhesins display different preferences with regard to the substituents' position and structure, which is consistent with earlier observations.[16] The recognition patterns of the type P_N and P_O adhesins are also markedly different to that of the *E. coli* class II adhesin. For *S. suis*, galabiosyl amides **5–10** (collection I) were poor inhibitors suggesting that *O*-galabiosides are preferred, possibly because the adhesins donate hydrogen bonds to galabiose O1. Hydrophobic (aromatic) galabioside aglycons (**11–27**, collection II) had, in general, a minor influence on the inhibitory powers compared to the reference methyl galabioside **47**, except for phenyl aglycons carrying an *ortho*-substituent (**12** and **21**) or an *m*-methoxy group (**11**) which were detrimental to inhibition. Introducing amides at galabiose C3′ (**34–42**) was also detrimental to inhibition of the type P_O adhesin, while it was well tolerated by the type P_N adhesin. Ureas at C3′ (**43–44**) were, not surprisingly, poor inhibitors of the type P_O adhesin. However, the ureas **43–44** were potent inhibitors of the type P_N adhesin. This correlates with the previously suggested Gal/GalNAc binding pocket at this site, which differentiates the P_N adhesin from the P_O adhesin.[16] Galabiose derivatives modified at O2′ with alkyl groups (**48–51**) appeared to be accepted by the type P_N adhesin. Interestingly, O2′-methoxymethyl substitution (**51**) provided one of the two best inhibitors against this adhesin, indicating the proximity of a hydrogen bond donor in the adhesin. Galabiosides carrying alkoxy-substituents at C3′ (**52–64**) were all relatively poor inhibitors of both *S. suis* adhesins.

The screening experiments against the two *S. suis* adhesins were further confirmed by selecting the ten best inhibitors and eight poorest inhibitors against each *S. suis* adhesin for refined evaluations in triplicate (Table 2). The refined evaluation established the IC$_{50}$ values of the two best inhibitors, the C3′-phenylurea **44** and the O2′-methoxymethyl **51**, against the type P_N adhesin to be 30 and 50 nM, respectively, which is up to one order of magnitude better than the parent unsubstituted *p*-methoxyphenyl galabioside **45** (IC$_{50}$ 310 nM) and significantly better than the previously reported best small-molecule inhibitor against this adhesin, the natural globotriose trisaccharide (IC$_{50}$ 190 nM).[16] The high affinities of **44** and **51** are extraordinary within the field of small-molecule inhibition of lectins. The synthesis of further galabiose collections modified with *O*-alkyl or alkoxymethyl substituents at O2′ or with ureas at C3′ thus emerges as an attractive route towards improved inhibitors. An obvious extension of this result would also be to combine the substituents of **44** and **51** into one single novel inhibitor, which would be significantly more potent provided that the affinity-

Table 2 IC$_{50}$ values for the 10 best and 8 poorest inhibitors of the adhesins from *S. suis* strains type P_N and type P_O

	IC$_{50}$/µM *S. suis* P_N	Range	IC$_{50}$/µM *S. suis* P_O	Range
5	5.2	3.9–7.8		
12	4.4	2.0–7.8		
13			0.42	0.31–0.63
15	0.20	0.16–0.31		
19			0.31	0.31
22			0.42	0.31–0.63
23			0.31	0.31
24			0.42	0.31–0.63
25			0.21	0.16–0.31
26			0.31	0.31
33	15.6	15.6		
35			54.7	31.3–62.5
37			52.1	31.3–62.5
38			20.8	15.6–31.3
39	0.16	0.08–0.31		
40			62.5	62.5
41	0.32	0.16–0.63	41.7	31.3–62.5
42			62.5	62.5
43	0.18	0.08–0.31	62.5	62.5
44	0.03	0.02–0.04		
45	0.18	0.08–0.31	0.31	0.31
47	0.63	0.63	0.63	0.63
49			31.3	31.3
50	0.18	0.08–0.31		
51	0.05	0.04–0.08		
56	6.5	3.9–7.8		
57	10.4	7.8–15.6		
58	15.6	15.6		
61	7.8	7.8		
64	10.4	7.8–15.6		

enhancing effects of each substituent are additive. Furthermore, displaying **44** or **51**, or a combination of these two inhibitors, on a multivalent scaffold would most likely result in more powerful inhibitors as multivalent inhibitors are known to be particularly efficient against the *S. suis* adhesins.[20]

The results with the type P_O adhesin were less impressive as only marginal affinity enhancements, compared to the known references **46–47**, were obtained. Clearly, other strategies have to be considered for the development of inhibitors against this adhesin. From a drug development perspective, it would of course be desirable to find one inhibitor with high affinity against both *S. suis* adhesins. However, this appears to be a formidable challenge in light of the results reported herein. Possibly, chemical modifications at positions other than C1 and C3′ of the galabiose disaccharide will be required to find an efficient inhibitor against both adhesins.

Structure–activity relationships for the *E. coli* class II PapG adhesin and the adhesin from *S. suis* type P_O

In order to develop a quantitative structure–activity relationship using multivariate data analysis, the four carbohydrate collections were characterised with molecular descriptors using the MOE software.[31] The 2D molecular descriptors included described properties such as size, lipophilicity, flexibility and hydrogen-bonding capabilities (see Table 3). The affinity of the carbohydrates as measured by log K_d and log IC$_{50}$ for the *E. coli* adhesin PapGII and the *S. suis* type P_O adhesin, respectively, were related to the various molecular descriptors by means of partial least-squares projections to latent structures (PLS).[32]

A PLS model was calculated including compounds **5, 8, 10–17, 19–20, 22–24, 26–27, 33–35, 39–48, 51** and **53–54** using all descriptors and log K_d for the PapGII adhesin as the response. After variable selection leaving 34 molecular descriptors as predictor variables (X), the model explained 78% ($R^2Y = 0.78$) of the total variation in the response data (Y) and was able to predict 68% ($Q^2 = 0.68$) of the response variation according to cross-validation. The predictive properties of the model were

Table 3 List of structural descriptors used for characterisation of galabiosides and regression coefficients for important factors in local PLS models for galabioside substituents in C1 and C3′ when biologically evaluated against *Escherichia coli* adhesin PapG type II and *Streptococcus suis* adhesin type P_O

	Abbreviation	Descriptors	*S. suis* type P_O		*E. coli* PapG	
			C1	C3′	C1	C3′
1	diameter	Molecular diameter	0.030			
2	radius	Molecular radius	0.016			
3	VDistEq	Vertex distance equation	0.013			
4	VDistMa	Vertex distance magnitude				
5	weinerPath	Weiner path number	−0.029			
6	weinerPol	Weiner polarity number				
7	a_aro	Number of aromatic atoms			0.052	
8	b_ar	Number of aromatic bonds			0.053	
9	b_rotN	Number of rotatable bonds	−0.058			
10	b_rotR	Fraction of rotatable bonds	−0.050	0.082	−0.061	0.092
11	chi0v	Atomic valence connectivity index				
12	chi0v_C	Carbon valence connectivity index				
13	chi1v	Atomic valence connectivity index				
14	chi1v_C	Carbon valence connectivity index				
15	Weight	Molecular weight				
16	chi0	Atomic connectivity index	−0.033			
17	chi0_C	Carbon connectivity index				
18	chi1	Atomic connectivity index				
19	chi1_C	Carbon connectivity index			0.053	
20	FCharge	Sum of formal charges				0.045
21	VAdjEq	Vertex adjacency equation				
22	VAdjMa	Vertex adjacency magnitude				
23	zagreb	Zagreb index				
24	balabanJ	Balaban connectivity index	−0.033		−0.078	
25	Q_PC+	Total positive partial charge		0.029	0.058	−0.030
26	Q_PC-	Total negative partial charge		−0.029	−0.062	0.029
27	Q_RPC+	Relative positive partial charge				
28	Q_RPC-	Relative negative partial charge		−0.010	−0.059	0.021
29	Q_VSA_FHYD	Fractional hydrophobic van der Waals surface area		0.008		−0.008
30	Q_VSA_FNEG	Fractional negative van der Waals surface area			0.062	
31	Q_VSA_FPNE	Fractional polar negative van der Waals surface area		−0.002		0.064
32	Q_VSA_FPOL	Fractional polar van der Waals surface area		−0.008		0.008
33	Q_VSA_FPOS	Fractional positive van der Waals surface area			−0.062	
34	Q_VSA_FPPO	Fractional polar positive van der Waals surface area	−0.042	−0.016		−0.096
35	Q_VSA_HYD	Total hydrophobic van der Waals surface area				
36	Q_VSA_NEG	Total negative van der Waals surface area				
37	Q_VSA_PNEG	Total polar negative van der Waals surface area		−0.038		0.039
38	Q_VSA_POL	Total polar van der Waals surface area		−0.104		−0.052
39	Q_VSA_POS	Total positive van der Waals surface area			−0.071	
40	Q_VSA_PPOS	Total polar positive van der Waals surface area	−0.099	−0.188		−0.200
41	Kier1	Kappa shape index	−0,039			
42	Kier2	Kappa shape index	−0.043			
43	Kier3	Kappa shape index	−0.018			
44	KierA1	Alpha modified shape index			−0.054	
45	KierA2	Alpha modified shape index				
46	KierA3	Alpha modified shape index				
47	KierFlex	Flexibility index		−0.018	−0.052	0.007
48	apol	Atomic polarizabilities				
49	bpol	Atomic polarizabilities				
50	mr	Molecular refractivity				
51	a_acc	Number of hydrogen bond acceptors	−0.051	0.116	0.044	0.058
52	a_acid	Number of acidic atoms		−0.008		−0.074
53	a_base	Number of basic atoms				
54	a_don	Number of hydrogen bond donors	−0.109	−0.356	−0.140	−0.197
55	a_hyd	Number of hydrophobic atoms				
56	vsa_acc	van der Waals surface areas of hydrogen bond acceptors	−0.044	−0.006		
57	vsa_acid	van der Waals surface areas of acidic atoms		−0.008		−0.074
58	vsa_base	van der Waals surface areas of basic atoms				
59	vsa_don	van der Waals surface areas of hydrogen bond donors	−0.105	−0.171	−0.140	−0.174
60	vsa_hyd	van der Waals surface areas of hydrophobic atoms				0.025
61	vsa_other	van der Waals Surface Areas of other atoms	−0.058	−0.217		−0.210
62	vsa_pol	van der Waals surface areas of polar atoms				
63	SlogP	Log of the octanol/water partition coefficient	0.109	0.008	0.100	0.116
64	SMR	Molecular refractivity				
65	TPSA	Total polar surface area	−0.080	−0.052	−0.050	−0.096
66	density	Molecular mass density			−0.049	
67	vdw_area	van der Waals surface area	−0.029			
68	vdw_vol	van der Waals volume				
69	logP(o/w)	Log of the octanol/water partition coefficient	0.074	0.009	0.084	0.085

further validated using an independent test set which included three carbohydrates from collection I (**6, 7, 9**), three from collection II (**18, 21, 23**), one from collection III (**25**), three from collection IV (**36–38**) and one C2′ substituted compound **50** (Fig. 2a). The model was able to predict the affinity of the test set compounds in an excellent way with a root mean square prediction error (RMSEP) of 0.49. Only one compound (**23**) was poorly predicted by the model. It was predicted to have a rather low affinity with a K_d of 350 μM, while the experimentally determined value was 150 μM.

To further evaluate two of the positions that were varied, C1 and C3′, two local PLS-models were created using compounds **5–27** and **45–47** for the anomeric position and **33–44** and **53–54** for the C3′ position. The number of substances with variation in

RMSEP = 0,49

RMSEP = 0,66
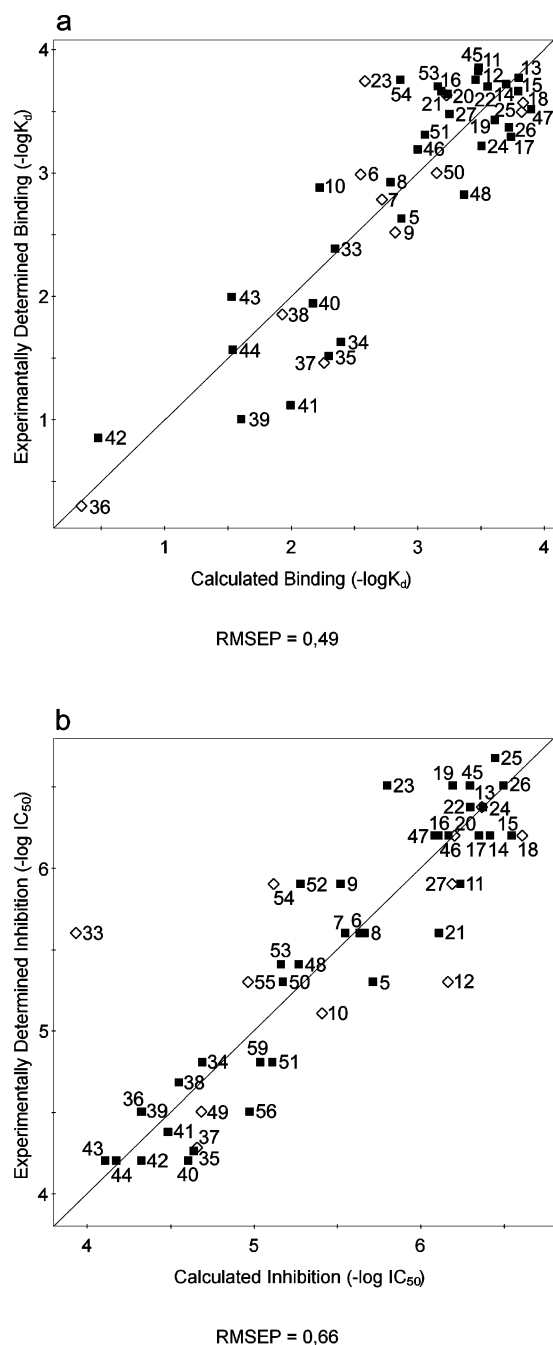
Fig. 2 Calculated response values for galabiosides (■) using the two different QSAR *versus* the experimental values for a) the binding affinity to *E. coli* adhesin PapG type II expressed as −log K_d ($R^2 Y = 0.78$, $Q^2 = 0.68$) and b) the inhibition of *S. suis* adhesin type P_O expressed as −log IC_{50} ($R^2 Y = 0.89$, $Q^2 = 0.75$). Both models were validated with an independent set of diverse galabiosides (◇); for chemical structures see Table 1.

the C2′ position were too few (**48, 50–51**) to be able to create a representative model. Variables not related to the response were removed by means of filtering. Two models with 20 and 23 important factors were retrieved for the anomeric and the C3′ position, respectively (see Table 3). For the anomeric position it could be further verified that aromatic substituents are important for affinity to the PapGII adhesin since regression coefficients for variables describing aromaticity and lipophilicity (a_aro, b_ar, SlogP and logP(o/w)) were positively correlated with the response. Coefficients related to flexibility (KierFlex, b_rotR) were negatively correlated indicating that groups with a high degree of freedom are unfavourable for binding (*cf.* **9** and **46**). In addition, it could be seen that the presence of either hydrogen bond donors or acceptors on the anomeric substituent was strongly correlated with the affinity. This could be seen in the poor affinity for inhibitors containing an amide functionality with hydrogen bond donation capacities adjacent to C1 (collection I) in comparison with the relatively high affinity for inhibitors with only hydrogen bond accepting properties at the same position (collection II and III). For the C3′ position it could be confirmed that replacing the ether functionality with a hydrogen bond donating amide is detrimental to binding ability since the presence of hydrogen bond acceptors was positively correlated and the presence of donors was negatively correlated with the response. Furthermore, positively correlated coefficients for flexibility indicate that a higher degree of freedom might be necessary in order to achieve the correct positioning of the substituent.

A schematic summary of the structure–activity relationships for the PapGII adhesin is shown in Fig. 3a. The shallow pocket formed by Arg170, Trp107, and Asp108, which is seen in the
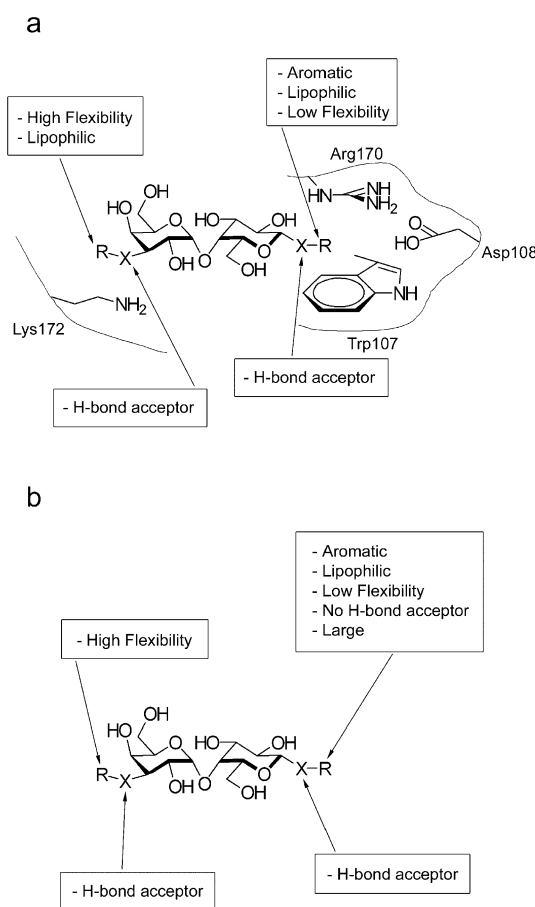
Fig. 3 a) Graphic summary of the structure–activity relationship of galabioses **5, 8, 10–17, 19–20, 22–24, 26–27, 33–35, 39–48, 51** and **53–54** in binding to the PapGII adhesin. Amino acids shown are in the proximity of the galabiose substituents according to the crystal structure of the adhesin–globotetraose complex.[19] b) Graphic summary of the structure–activity relationship of galabiose inhibitors **5–9, 11, 14–17, 19, 21–26, 34–36, 38–48, 50–53, 56** and **59** of the *S. suis* P_O adhesin.

crystal structure of PapGII together with a tetrasaccharide,[19] could explain the increase in affinity provided by C1 substituents with low flexibility. The preference for aromatic groups in the same pocket could derive from Π-stacking or cation-Π interactions from Trp107 and Arg170. The hydrogen bonding properties seen at both O1 and O3′ indicate the presence of important hydrogen bonds from Lys172 to O3′, as seen in the crystal structure, and from either residue Arg170 or Trp107 to the neighbouring O1. Flexibility in inhibitors is not normally beneficial for entropic reasons and the prediction by the model that the inhibitors should have flexible substituents at C3′ probably reflects that the geometric requirements on rigid substituents are higher, as rigid substituents are less adaptable to the steric requirements of the protein binding site. Presumably, a rigid substituent properly designed to sterically match the binding site of the PapGII adhesin would improve the affinity.

Relating the aforementioned molecular descriptors for compounds **5–9, 11, 14–17, 19, 21–26, 34–36, 38–48, 50–53, 56** and **59** to IC$_{50}$ values (from the refined measurements in Table 2 when applicable) for *S. suis* adhesins P$_O$ and P$_N$ by using PLS gave, after variable selection, a prediction model for inhibition of the adhesin type P$_O$ with 38 variables describing 89% of the total variation in the response and $Q^2 = 0.75$. The predictive properties of the model were further validated using an independent test set, which included one compound from collection I (**10**), four from collection II (**12–13, 18, 20**), one from collection III (**27**), two from collection IV (**33 and 37**), one C2′ substituted compound (**49**) and two known galabiosides (**54 and 55**), Fig. 2b. The prediction of the test set gave good results, with the exception of compound **33**, with an RMSEP of 0.66. The galabioside **33**, however, is the only basic amine in the collection tested, which could explain the prediction difficulties for this compound. Excluding that object from the test set gave excellent prediction results, RMSEP = 0.44. No significant model for the adhesin type P$_N$ could be retrieved, maybe due to insufficient variation in the response. The galabiosides **57–58** and **60–64** were excluded, since the long and flexible side-chains in both of the positions varied made them difficult to model with the 2D descriptors that were used.

Local PLS models on galabiosides **5–27, 45–47** and **33–44, 52–56** for the anomeric and C3′ positions, respectively, resulted in two models with 22 important variables. The model for the anomeric position could further verify that substituents with low flexibility and high lipophilicity such as aromatic rings are beneficial for affinity. Both hydrogen bond accepting and donating capabilities are negatively correlated to the response, donors to a larger extent. The negatively correlated term for hydrogen bond donors is probably related to the C1 linkage position since good activity can be observed in all cases when donor substituents are present elsewhere (**16, 23**). The opposite can be said of the negatively correlated term for hydrogen bond acceptors where it seems that acceptors on positions other than the C1 linkage are unfavourable, as can be seen in the galabiosides with methoxy substituted aromatic rings (*e.g.* **11, 12**). The C3′ position model clarifies the importance of having the ether linkage intact. Amides with hydrogen bond donor coefficients are strongly negatively correlated, whereas hydrogen bond acceptor terms are positively correlated with affinity (*cf.* **52–55** with collection IV). A schematic summary of the structure–activity relationships is shown in Fig. 3b. This proposes that a good inhibitor of the *S. suis* adhesin type P$_O$ should be a galabioside with large aromatic and highly lipophilic aglycons, *e.g.* naphthyl galabiosides. In addition, a highly flexible group should be attached to a hydrogen bond acceptor at C3′. However, the prediction that a flexible group at C3′ is beneficial could be misleading, as discussed for the PapGII adhesin above, and a rigid substituent properly designed to sterically match the binding site of the P$_O$ adhesin could improve the affinity.

Two PLS models were obtained with the ability to predict the affinity of new galabiosides for the *E. coli* adhesin PapGII

and the *S. suis* adhesin type P$_O$ in an excellent fashion. In addition, local models for each position varied and provided quantitative structure–activity relationships for both adhesins. These relationships may be used to optimise the substituents further and constitute a base for future designed libraries where all positions will be varied at the same time in order to reveal interaction effects between the different substituents.

Conclusions

Four collections of galabiosides derivatised at C1 and C3′ have been synthesised aiming at enhanced affinity, compared to the parent galabioside disaccharide, for the *E. coli* class II PapG adhesin and the type P$_N$ and type P$_O$ adhesins from *S. suis*. The present study clearly shows that the *E. coli* class II PapG adhesin recognizes *m*- or *p*-methoxyphenyl galabiosides **11** and **45** with high affinity and specificity. Although various approaches towards galabiose derivatives carrying aromatic structures at C1 were evaluated (*i.e.* replacing the anomeric oxygen with an amido group or a sulfur atom or modifying the aromatic structure) no improvements in affinity for the adhesin were revealed. Furthermore, structural modifications at C3′ did not provide any significant affinity enhancements for the PapGII adhesin. Hence, the *m*- or *p*-methoxyphenyl galabiosides **11** and **45** constitute lead structures in future work towards agents targeting urinary tract infections. Remarkably potent inhibitors were discovered against one of the *S. suis* adhesins (type P$_N$, IC$_{50}$ down to 30 nM), which provide an ideal starting point for the further development of mono-, as well as multivalent, inhibitors of this adhesin. The PapGII preferentially bound to substituted phenyl galabiosides, while the P$_O$ preferentially bound *p*-methoxyphenyl galabiosides substituted with hydrogen bond accepting alkyl groups at O2′ or phenyl ureas at C3′. PLS models could accurately predict affinity-enhancing effects of substituents in binding to the *E. coli* PapGII and *S. suis* type P$_O$ adhesins, which is of value for the design of further improved inhibitors.

Experimental

Synthesis

General methods. All non-aqueous reactions were run in septum-capped, oven-dried flasks under Ar (1 atm). CH$_2$Cl$_2$ was dried by distillation from CaH$_2$ and Et$_2$O was distilled from Na. Organic solutions were concentrated by rotary evaporation with a bath temperature at or below 40 °C. Flash chromatography was performed on Grace Amicon Silica gel 60 (35–70 μm) and TLC was performed on Kieselgel 60 F$_{254}$ plates (Merck). C18 cartridges were from IST Ltd, UK. NMR spectra were recorded with Bruker DRX-400 or ARX-300 instruments. Residual CHCl$_3$ or CD$_2$HOD were used as internal references at 7.27 and 3.31 ppm, respectively. ^{1}H-NMR spectral assignments were made based on COSY spectra. *J* values are given in Hz.

2,3,4,6-Tetra-*O*-acetyl-α-D-galactopyranosyl-(1→4)-2,3,6-tri-*O*-benzoyl-β-D-galactopyranosyl azide (3). To a solution of 2,3,4,6-tetra-*O*-acetyl-α-D-galactopyranosyl-(1→4)-2,3,6-tri-*O*-benzoyl-α-D-galactopyranosyl bromide **1**[22] (2.58 g, 2.96 mmol) in THF (100 mL) were added trimethylsilyl azide (0.55 mL, 4.15 mmol) and tetrabutylammonium fluoride (3.55 mL, 3.55 mmol, 1 M in THF) and the mixture was stirred for 24 h. The mixture was filtered through a silica column (2 : 1→2 : 3, heptane–EtOAc gradient) to give **3** (2.31 g, 92%); [a]$_D^{23}$ +91 (*c* 1.0 in CDCl$_3$); δ$_H$(300 MHz; CDCl$_3$) 8.10–7.95 (m, 6H, Ar–H), 7.65–7.36 (m, 9H, Ar–H), 5.71 (dd, 1H, *J* 10.6, 12.5, H-2), 5.50 (m, 2H, H-3′, H-4′), 5.42 (dd, 1H, *J* 2.8, 10.5, H-3), 5.30–5.23 (m, 2H, H-1′, H-2′), 4.92 (d, 1H, *J* 8.6, H-1), 4.77 (dd, 1H, *J* 6.9, 11.5, H-6), 4.58–4.51 (m, 2H, H-5′, H-6), 4.49 (d, 1H, *J* 2.6, H-4), 4.23 (t, 1H, *J* 6.6, H-5), 3.83 (dd, 1H, *J* 7.5, 11.0, H-6′), 3.69 (dd, 1H, *J* 6.4, 11.0, H-′), 2.18, 2.11, 2.04, 1.87 (s, 3H each, OAc); δ$_C$(75 MHz; CDCl$_3$) 170.6, 170.2, 170.1, 169.8,

166.0, 165.9, 165.0, 133.8, 133.6, 133.5, 129.82, 129.75, 129.1, 128.8, 128.7, 128.6, 128.4, 98.0, 88.5, 74.8, 74.6, 73.1, 68.7, 68.2, 67.7, 67.35, 67.25, 62.1, 60.8, 20.8, 20.7, 20.6, 20.5; m/z (FAB) 870.2336 (M^+ + Na. $C_{41}H_{41}N_3O_{17}$Na requires 870.2334).

α-D-Galactopyranosyl-(1→4)-β-D-galactopyranosyl azide (4). To a solution of **3** (2.00 g, 2.36 mmol) in MeOH (150 mL) was added NaOMe (0.05 mL, 0.05 mmol, 1 M in MeOH) and the mixture was stirred for 18 h then 10% methanolic acetic acid was added until a neutral reaction was obtained on moist pH-paper. Concentration and flash chromatography (SiO$_2$, 66 : 33 : 4→50 : 50 : 4, CH$_2$Cl$_2$–MeOH–H$_2$O gradient) gave **4** (832 mg, 96%); $[a]_D^{23}$ +72 (c 1.0 in MeOH); δ_H(300 MHz; CD$_3$OD); 4.99 (d, 1H, J 3.6, H-1′), 4.56 (d, 1H, J 8.3, H-1), 4.22 (m, 1H, H-5′), 4.03 (d, J 2.4, H-4′), 3.93 (dd, 1H, J 1.0, 2.9, H-4), 3.87–3.71 (m, 7H), 3.57 (dd, 1H, J 3.0, 10.0), 3.45 (dd, 1H, J 8.3, 10.0); δ_C(75 MHz; CD$_3$OD) 103.5, 93.5, 80.5, 78.9, 75.5, 73.8, 73.2, 72.0, 71.8, 71.3, 63.5, 62.0; m/z (FAB) 390.1127 (M^+ + Na. $C_{12}H_{21}N_3O_{10}$Na requires 390.1125).

General procedure for the synthesis of compounds 5–10. A solution of **4** (15 mg, 0.041 mmol) in MeOH (0.7 mL) was hydrogenated (H$_2$, 1 atm, Pd/C 10%, cat) for 30 min. Na$_2$CO$_3$ (30 mg, 0.27 mmol) was added, followed by dropwise addition of a solution of the acid chloride or anhydride (0.41 mmol, 10 eq.) in THF (0.7 mL). After 30 min, the solution was filtered through Celite, concentrated and dissolved in water. The solution was applied to a C-18 cartridge (2 g), which was washed with water and eluted with MeOH–H$_2$O (2 : 1). Concentration and flash chromatography (SiO$_2$, CH$_2$Cl$_2$–MeOH–H$_2$O) gave **5–10**. ^{1}H-NMR and FAB-HRMS data are listed in Table 4.

General procedure for the synthesis of compounds 11–19. To a solution of **2**[22] (40 mg, 42 μmol) in dry CH$_2$Cl$_2$ (1.2 mL) at −20 °C was added the alcohol (84 μmol, 2 eq.) and TMSOTf (2 μL, 13 μmol). The reaction mixture was stirred for 30 min and Et$_3$N (0.1 mL) was added. The mixture was concentrated and flash chromatographed (SiO$_2$, heptane–EtOAc). Deacylation (2.0 mL, 0.01 M NaOMe in MeOH) overnight, followed by addition of 10% methanolic acetic acid until a neutral reaction was obtained on moist pH-paper, concentration, and flash chromatography (SiO$_2$, CH$_2$Cl$_2$–MeOH) gave **11–19**. ^{1}H-NMR and FAB-HRMS are listed in Table 4.

General procedure for the synthesis of compounds 20–22 and 24–27. To a solution of the alcohol (69 μmol, 1.5 eq.) in DMF (0.5 mL) was added NaH (2.9 mg, 74 μmol, 60% in mineral oil) and the mixture was stirred for 15 min. The resulting solution was added dropwise to a solution of **1** (40 mg, 46 μmol) in DMF. After 45 min, the reaction mixture was diluted with CH$_2$Cl$_2$ (5 mL), washed with sat'd NaHCO$_{3(aq.)}$ (2 mL), dried (Na$_2$SO$_4$), and flash chromatographed (SiO$_2$, heptane–EtOAc). Deacylation (2.0 mL, 0.01 M NaOMe in MeOH) overnight was followed by addition of 10% methanolic acetic acid until a neutral reaction was obtained on moist pH-paper. Concentration and flash chromatography (SiO$_2$, CH$_2$Cl$_2$–MeOH) gave **20–22** and **24–27**. ^{1}H-NMR and FAB-HRMS are listed in Table 4.

Methyl 3-azido-3-deoxy-2,4,6-tri-O-benzyl-1-thio-β-D-galactopyranoside (29). To a solution of **28**[25] (990 mg, 2.74 mmol) in MeOH (50 mL) was added NaOMe (0.1 mL, 1 M in methanol) and the solution was stirred overnight. Methanolic acetic acid (10%) was added until a neutral reaction was obtained on moist pH-paper and the mixture was concentrated. The residue was dissolved in DMF (10 mL), NaH (390 mg, 9.9 mmol, 60% in mineral oil) was added, and the mixture was stirred for 15 min, then cooled to 0 °C. Benzyl bromide (1.2 mL, 9.9 mmol) was added dropwise and the mixture was allowed to reach ambient temperature overnight. MeOH (5 mL) was added, the mixture was diluted with CH$_2$Cl$_2$ (100 mL), washed with sat'd NaHCO$_{3(aq.)}$ (50 mL), dried (MgSO$_4$), concentrated

and flash chromatographed (SiO$_2$, 2 : 1→2 : 3, heptane–EtOAc gradient) to give **29** (1.19 g, 86%); $[a]_D^{23}$ −42 (c 0.9 in CHCl$_3$); δ_H(300 MHz; CDCl$_3$); 7.48 (m, 2H, Ar–H), 7.37–7.28 (m, 13H, Ar–H), 4.97/4.78 (ABq, 2H, J 9.9, CH$_2$), 4.88/4.60 (ABq, 2H, J 11.4, CH$_2$), 4.47/4.44 (ABq, 2H, J 11.7, CH$_2$), 4.37 (d, 1H, J 9.4, H-1), 3.93 (d, 1H, J 2.7, H-4), 3.80 (t, 1H, J 9.6, H-2), 3.60 (m, 3H, H-5, 2 × H-6), 3.54 (dd, 1H, J 3.0, 9.7, H-3), 2.25 (s, 3H, CH$_3$); δ_C(75 MHz; CDCl$_3$) 138.08, 138.07, 137.7, 137.4, 128.69, 128.67, 128.64, 128.57, 128.49, 128.46, 128.44, 128.40, 128.35, 128.29, 128.26, 128.2, 128.1, 128.04, 128.01, 127.98, 127.89, 127.87, 127.86, 127.70, 127.68, 85.9, 76.6, 75.2, 75.09, 75.06, 73.53, 73.52, 68.2, 67.0, 12.8; m/z (FAB) 528.1940 (M^+ + Na. $C_{28}H_{31}N_3O_4$SNa requires 528.1933).

4-Methoxyphenyl (3-azido-3-deoxy-2,4,6-tri-O-benzyl-α-D-galactopyranosyl)-(1→4)-2,3,6-tri-O-benzoyl-β-D-galactopyranoside (31). To a mixture of **29** (55 mg, 0.11 mmol), **30**[22] (50 mg, 84 μmol) and N-iodosuccinimide (48 mg, 0.22 mmol) were added CH$_2$Cl$_2$ (1.0 mL) and Et$_2$O (2.0 mL) and the solution was cooled to −50 °C. TMSOTf (3 μL, 17 μmol) was added and the mixture was stirred for 1 h. Triethylamine (0.5 mL) was added and the mixture was stirred for another hour at −50 °C, then allowed to reach ambient temperature, diluted with CH$_2$Cl$_2$ (20 mL), washed with 10% Na$_2$S$_2$O$_{3(aq.)}$ (10 mL) and sat'd NaHCO$_{3(aq.)}$ (10 mL), dried (MgSO$_4$), and concentrated. Flash chromatography (SiO$_2$, 3 : 1 heptane–EtOAc) gave **31** (82 mg, 93%); $[a]_D^{23}$ +75 (c 1.0 in CHCl$_3$); δ_H(300 MHz; CDCl$_3$); 8.07–7.95 (m, 6H, Ar–H), 7.66–7.20 (m, 24H, Ar–H), 6.97 (m, 2H, OPhOMe), 6.69 (m, 2H, OPhOMe), 6.00 (dd, 1H, J 7.7, 10.5, H-2), 5.29 (dd, 1H, J 2.8, 10.5, H-3), 5.17 (d, 1H, J 7.7, H-1), 4.97 (d, 1H, J 3.2, H-1′), 4.86–4.69 (m, 5H, 2 × H-6), 4.55–4.43 (m, 3H, H-4, H-5′), 4.22–4.15 (m, 4H, H-3′, H-5), 4.07 (m, 1H, H-4′), 4.04 (dd, 1H, J 3.2, 10.7, H-2′), 3.74 (s, 3H, OMe), 3.44 (t, 1H, J 8.7, H-6′), 3.10 (dd, 1H, J 4.8, 8.5, H-6′); δ_C(100 MHz; CDCl$_3$) 166.9, 166.5, 165.8, 156.0, 151.6, 138.64, 138.62, 137.8, 133.9, 133.71, 133.69, 130.4, 130.20, 130.17, 130.1, 129.9, 129.4, 128.94, 128.91, 128.86, 128.78, 128.76, 128.7, 128.6, 128.4, 128.1, 128.0, 119.2, 114.8, 101.3, 100.3, 76.4, 76.2, 75.9, 74.6, 74.0, 73.4, 69.91, 69.86, 67.7, 63.2, 61.7, 56.0; m/z (FAB) 1078.3743 (M^+ + Na. $C_{61}H_{57}N_3O_{14}$Na requires 1078.3738).

4-Methoxyphenyl (3-azido-3-deoxy-2,4,6-tri-O-benzyl-α-D-galactopyranosyl)-(1→4)-β-D-galactopyranoside (32). To a solution of **31** (318 mg, 0.43 mmol) in MeOH (10 mL) was added NaOMe (0.10 mL, 1 M in MeOH) and the reaction mixture was stirred overnight, then 10% methanolic acetic acid was added until a neutral reaction was obtained on moist pH-paper. Concentration and flash chromatography (SiO$_2$, toluene–acetone, 4 : 1) gave **32** (201 mg, 89%); $[a]_D^{25}$ −8 (c 1.0 in CHCl$_3$); δ_H(400 MHz; CDCl$_3$); 7.40–7.31 (m, 15H, Ar–H), 6.99 (m, 2H, OPhOMe), 6.81 (m, 2H, OPhOMe), 4.89/4.64 (ABq, 2H, J 11.6, CH$_2$), 4.89/4.53 (ABq, 2H, J 11.4, CH$_2$), 4.89 (m, 1H, H-1′), 4.71 (d, 1H, J 7.5, H-1), 4.46/4.40 (ABq, 2H, J 11.4, CH$_2$), 4.20 (m, 1H, H-5′), 4.04 (dd, 1H, J 3.4, 10.6, H-2′), 3.98 (dd, 1H, J 2.8, 10.6, H-3′), 3.94 (m, 1H, H-4), 3.88 (d, 1H, J 11.9, OH), 3.83 (m, 1H, H-4′), 3.77 (m, 5H, 2 × H-6, OMe), 3.70 (m, 2H, H-2, H-5), 3.53 (t, 1H, J 9.5, H-6′), 3.45 (m, 1H, H-3), 3.25 (dd, 1H, J 3.7, 9.6, H-6′), 2.94 (t, 1H, J 6.7, OH), 2.15 (s, 1H, OH); δ_C(100 MHz; CDCl$_3$) 155.8, 151.6, 137.79, 137.78, 136.9, 129.3, 129.2, 129.0, 128.91, 128.87, 128.64, 128.61, 128.57, 119.0, 114.9, 102.8, 100.0, 81.0, 76.07, 76.05, 75.7, 74.9, 74.5, 74.3, 74.2, 72.3, 71.6, 69.7, 62.1, 61.0, 56.1; m/z (FAB) 766.2956 (M^+ + Na. $C_{40}H_{45}N_3O_{11}$Na requires 766.2952).

4-Methoxyphenyl (3-amino-3-deoxy-α-D-galactopyranosyl)-(1→4)-β-D-galactopyranoside (33). A solution of **32** (30 mg, 40 μmol), HCl$_{(aq.)}$ (5 μL, conc.), and Pd/C (10%, 10 mg) in MeOH (0.7 mL) was hydrogenated (H$_2$, 1 atm) for 30 min. The solution was filtered through Celite, concentrated, re-dissolved in H$_2$O, and applied to a C-18 cartridge (2 g). The cartridge

Table 4 ^{1}H NMR and FAB-HRMS data of compounds **5–27** and **33–44**

	δ_H(300 MHz; CD$_3$OD)	m/z (FAB) (M$^+$ + Na) required/found
5	7.91 (m, 2H, Ar), 7.58–7.45 (m, 3H, Ar), 5.13 (d, 1H, J 8.9, H-1), 5.03 (d, 1H, J 3.6, H-1′), 4.31 (t, 1H, J 6.2, H-5′)	468.1482/468.1482
6	7.89 (m, 2H, Ar), 7.00 (m, 2H, Ar), 5.11 (d, 1H, J 8.8, H-1), 5.03 (d, 1H, J 3.4, H-1′), 4.31 (t, 1H, J 6.8, H-5′)	498.1587/498.1583
7	7.55 (m, 1H, Ar), 5.08 (m^a, 1H, H-1), 5.02 (d, 1H, J 3.7, H-1′), 4.23 (t, 1H, J 6.0, H-5′)	540.1105/540.1107
8	7.53 (m, 2H, Ar), 7.18 (m, 1H, Ar), 5.10 (d, 1H, J 8.9, H-1), 5.03 (d, 1H, J 3.8, H-1′), 4.29 (t, 1H, J 6.8, H-5′)	504.1293/504.1300
9	5.01 (d, 1H, J 3.8, H-1′), 4.88 (d, 1H, J 8.3, H-1), 4.26 (t, 1H, J 5.6, H-5′), 2.29 (m, 2H, CH$_2$), 1.14 (t, 3H, J 7.6, CH$_3$)	420.1481/420.1501
10	8.01 (m, 1H, Ar), 6.67 (m, 2H, Ar), 5.12 (m^a, 1H, H-1), 5.02 (d, 1H, J 2.6, H-1′), 4.34 (t, 1H, J 6.7, H-5′)	528.1693/528.1697
11	7.17 (m, 1H, Ar), 6.69 (m, 2H, Ar), 6.60 (m, 1H, Ar), 5.02 (m^a, H-1′), 4.93 (d, 1H, J 7.4, H-1), 4.33 (t, 1H, J 5.9, H-5′)	471.1478/471.1471
12	7.16 (m, 1H, Ar), 7.02 (m, 2H, Ar), 6.90 (m, 1H, Ar), 5.02 (d, J 1.7, H-1′), 4.93 (d, 1H, J 7.6, H-1), 4.34 (t, 1H, J 6.4, H-5′)	471.1478/471.1482
13	7.29 (m, 2H, Ar), 7.10 (m, 1H, Ar), 7.02 (m, 1H, Ar), 5.01 (m^a, 1H, H-1′), 4.96 (d, 1H, J 7.4, H-1), 4.33 (t, 1H, J 5.8, H-5′)	441.1373/441.1359
14	7.08 (m, 2H, Ar), 6.99 (m, 2H, Ar), 5.01 (m^a, 1H, H-1′), 4.90 (d, 1H, J 7.5, H-1), 4.32 (t, 1H, J 5.8, H-5′)	455.1529/455.1520
15	7.78 (m, 3H, Ar), 7.49–7.28 (m, 4H, Ar), 5.12 (d, 1H, J 7.5, H-1), 5.03^a (m, 1H, H-1′), 4.34 (t, 1H, J 5.6, H-5′)	491.1529/491.1525
16	7.34–7.21 (m, 3H, Ar), 6.97 (m, 1H, Ar), 6.37 (m, 1H, Ar), 5.02 (d, 1H, J 2.8, H-1′), 4.87 (d, 1H, J 7.5, H-1), 4.36 (t, 1H, J 6.6, H-5′)	480.1482/480.1490
17	7.45–7.26 (5, 2H, Ar), 4.97 (d, 1H, J 1.7, H-1′), 4.91 (AB, 1H, J 11.7, CH$_2$), 4.69 (AB, 1H, J 11.7, CH$_2$), 4.40 (m^a, 1H, H-1), 4.31 (t, 1H, J 6.5, H-5′)	455.1529/455.1526
18	4.97 (m^a, 1H, H-1′), 4.40 (d, 1H, J 7.5, H-1), 4.34 (t, 1H, J 6.6, H-5′), 1.96 (m, 2H, CH$_2$), 1.77 (m, 2H, CH$_2$), 1.55 (m, 1H, CH$_2$), 1.47–1.20 (m, 5H, CH$_2$)	447.1842/447.1849
19	5.01 (d, 1H, J 2.8, H-1′), 4.93 (d, 1H, J 7.5, H-1), 4.29 (t, 1H, J 6.4, H-5′)	531.0901/531.0901
20	7.97 (m, 2H, Ar), 7.16 (m, 2H, Ar), 5.06 (d, 1H, J 7.5, H-1), 5.01 (d, 1H, J 3.0, H-1′), 4.31 (t, 1H, J 5.9, H-5′)	499.1428/499.1432
21	7.78 (m, 1H, Ar), 7.54 (m, 1H, Ar), 7.37 (m, 1H, Ar), 7.14 (m, 1H, Ar), 5.01 (d, 1H, J 1.8, H-1′), 4.92 (d, 1H, J 7.5, H-1), 4.32 (t, 1H, J 6.6, H-5′)	499.1428/499.1426
22	8.22 (m, 2H, Ar), 7.25 (m, 2H, Ar), 5.11 (d, 1H, J 7.5, H-1), 5.01 (d, 1H, J 3.4, H-1′), 4.30 (t, 1H, J 6.1, H-5′)	486.1224/486.1222
23	7.45 (m, 2H, Ar), 7.06 (m, 2H, Ar), 5.01 (d, 1H, J 1.8, H-1′), 4.90 (d, 1H, J 7.5, H-1), 4.32 (t, 1H, J 5.9, H-5′)	498.1587/498.1584
24	7.55 (m, 2H, Ar), 6.90 (m, 2H, Ar), 4.87 (d, 1H, J 3.8, H-1′), 4.38 (d, 1H, J 9.3, H-1)	487.1250/487/1251
25	7.59 (m, 2H, Ar), 7.30 (m, 3H, Ar), 4.93 (d, 1H, J 3.8, H-1′), 4.58 (d, 1H, J 9.0, H-1)	457.1144/457.1137
26	7.49 (m, 2H, Ar), 7.15 (m, 2H, Ar), 4.90 (d, 1H, J 3.8, H-1′), 4.49 (d, 1H, J 9.2, H-1)	471.1301/471.1294
27	7.91 (m, 1H, Ar), 7.74 (m, 1H, Ar), 7.59 (m, 1H, Ar), 7.42 (m, 1H, Ar), 4.95 (d, 1H, J 2.9, H-1′), 4.89 (d, 1H, J 9.6, H-1), 4.11 (t, 1H, J 6.5)	515.1199/515.1208
33	5.06 (d, 1H, J 3.6, H-1′), 4.85 (d, 1H, J 7.1, H-1), 4.43 (t, 1H, J 6.3, H-5′), 3.53 (dd, 1H, J 1.7, 10.8, H-3′)	470.1638/470.1642
34	5.03 (d, 1H, J 3.8, H-1′), 4.83 (d, 1H, J 7.6, H-1), 4.44 (t, 1H, J 6.5, H-5′), 4.23 (dd, 1H, J 2.9, 11.4, H-3′), 2.02 (s, 3H, NHAc)	512.1744/512.1744
35	5.08 (d, 1H, J 3.8, H-1′), 4.86 (d, 1H, J 7.6, H-1), 4.44 (t, 1H, J 6.1, H-5′), 4.23 (dd, 1H, J 2.9, 11.4, H-3), 2.29 (q, 2H, J 7.7, CH$_2$), 1.15 (t, 3H, J 7.6, CH$_3$)	526.1900/526.1893
36	5.04 (d, 1H, J 3.7, H-1′), 4.82 (d, 1H, J 7.6, H-1), 4.43 (t, 1H, J 6.8, H-5′), 4.23 (dd, 1H, J 2.9, 11.4, H-3), 2.60 (m, 4H, J 7.7, CH$_2$)	570.1799/570.1786
37	7.89 (m, 2H, Ar–H), 7.50 (m, 3H, Ar–H), 5.10 (d, 1H, J 3.7, H-1′), 4.84 (d, 1H, J 7.7, H-1), 4.49 (m, 2H, H-3′, H-5′)	574.1900/574.1895
38	7.86 (m, 2H, Ar–H), 6.98 (m, 2H, Ar–H), 5.09 (d, 1H, J 3.7, H-1′), 4.84 (d, 1H, J 7.6, H-1), 4.51 (t, 1H, J 5.8, H-5′), 4.45 (dd, 1H, J 2.9, 11.4, H-3′), 3.85 (s, 3H, OMe)	604.2006/604.2021
39	7.06 (m, 2H, Ar–H), 6.64 (m, 1H, Ar–H), 5.09 (d, 1H, J 3.7, H-1′), 4.84 (d, 1H, J 7.6, H-1), 4.52 (t, 1H, J 6.1, H-5′), 4.44 (dd, 1H, J 2.9, 11.4, H-3′)	634.2112/634.2101
40	7.54 (m, 2H, Ar–H), 7.15 (m, 1H, Ar–H), 5.09 (d, 1H, J 3.8, H-1′), 4.84 (d, 1H, J 7.6, H-1), 4.52 (t, 1H, J 5.9, H-5′), 4.43 (dd, 1H, J 2.9, 11.4, H-3′)	610.1712/610.1699
41	8.78 (m, 1H, Ar–H), 8.40 (m, 1H, Ar–H), 8.28 (m, 1H, Ar–H), 7.73 (m, 1H, Ar–H), 5.10 (d, 1H, J 3.8, H-1′), 4.84 (d, 1H, J 7.7, H-1), 4.53 (t, 1H, J 6.7, H-5′), 4.49 (dd, 1H, J 2.9, 11.4, H-3′)	619.1751/619.1774
42	7.89 (m, 1H, Ar–H), 7.52 (m, 3H, Ar–H), 5.06 (d, 1H, J 3.7, H-1′), 4.83 (d, 1H, J 7.6, H-1), 4.50 (t, 1H, J 6.1, H-5′), 4.38 (dd, 1H, J 2.8, 11.3, H-3′)	618.1799/618.1791
43	5.02 (d, 1H, J 3.7, H-1′), 4.81 (d, 1H, J 7.5, H-1), 4.40 (t, 1H, J 5.7, H-5′), 4.10 (dd, 1H, J 3.0, 11.2, H-3′), 3.15 (q, 2H, J 7.2, CH$_2$), 1.09 (t, 3H, J 7.2, CH$_2$CH_3)	541.2009/541.2011
44	7.35 (m, 2H, Ar–H), 7.23 (m, 2H, Ar–H), 6.95 (m, 1H, Ar–H), 5.06 (d, 1H, J 3.8, H-1′), 4.83 (d, 1H, J 7.6, H-1), 4.45 (t, 1H, J 5.6, H-5′), 4.49 (dd, 1H, J 3.0, 11.2, H-3′)	589.2009/589.1995

^{a} Virtual long-range couplings.

was washed with water, eluted with a 10–50% MeOH gradient, and concentrated to give **33** (18 mg, 93%). ^{1}H-NMR and FAB-HRMS are listed in Table 4.

General procedure for the synthesis of 34–44. A solution of **32** (30 mg, 40 µmol) in MeOH (0.7 mL) HCl$_{(aq.)}$ (5 µL, conc.), and

Pd/C (10%, 10 mg) in MeOH (0.7 mL) was hydrogenated (H$_2$, 1 atm) for 30 min. Na$_2$CO$_3$ (30 mg, 0.27 mmol) was added, followed by a solution of an acid chloride, acid anhydride, or isocyanate (0.41 mmol, 10 eq.) in THF (0.7 mL). After 30 min, the solution was filtered through Celite, concentrated, dissolved in 10% MeOH (9 : 1), and applied to a C-18 cartridge

(2 g). The cartridge was washed with water, then eluted with 50% MeOH. Concentration and flash chromatography (SiO$_2$, CH$_2$Cl$_2$–MeOH–H$_2$O) gave **34–44**. ^{1}H-NMR and FAB-HRMS are listed in Table 4.

Surface plasmon resonance experiments

Surface plasmon resonance studies of binding of compounds **5–46** to the class II PapG adhesin were performed as described earlier.[21] The binding data were analysed using the software Scrubber.[28]

Hemagglutination inhibition experiments

Bacteria were grown overnight at 37 °C at 5% CO$_2$-incubator. The bacteria were harvested by centrifugation, 5000 × g, 15 min, +4 °C, and washed twice with PBS. The hemagglutination activities were titrated and the lowest bacterial densities causing agglutination were used for the inhibition studies. Twofold dilutions of the inhibitors were tested and the results were observed after incubation on ice for two hours. A first screen was done once with strain 628 (type P$_N$) and strain 836 (type P$_O$). The hemagglutination type was verified by using galactose and N-acetylgalactosamine as inhibitors. Ten strong inhibitors and eight poor inhibitors were selected for refined evaluation in triplicate. The results are presented as the average of three individual determinations and the range of the inhibitory values is shown.

Computational methods

Characterisation of oligosaccharides. The structures were generated using the MOE software carbohydrate and molecule builder interface and energy minimized with the MMFF94 merck and PEF95SAC carbohydrate force fields and an implicit solvent electrostatic correction model as implemented in MOE.[31] Characterisation of the carbohydrates was done by the MOE software and the molecular descriptors include properties of size, lipophilicity, polarizability, charge, flexibility, rigidity and hydrogen-bonding capacities (Table 3).

Data analysis methods. The binding affinities of the oligosaccharides as measured by $-\log K_d$ and $-\log$ IC$_{50}$ for PapGII and S. suis adhesin type P$_O$ respectively were related to the molecular descriptors by means of partial least squares projection to latent structures (PLS)[32] using the statistical software Simca.[33] The number of significant components was decided by cross-validation using the default set up.[33] Generally, variable selection was accomplished by excluding all variables with a variable importance in the projection value (VIP) below 1, hence keeping the variables inducing an increase in the predictive power of the model. The VIP value is a weighted sum of squares of the PLS weights, w, taking into account the amount of explained Y variance of each PLS dimension.[34]

The two prediction models were validated using an independent test set. The local PLS models were validated using a permutation test where the order of the response (Y) was randomly permutated 30 times. By plotting the explanatory power (R^2) and the predictive power (Q^2) of the mutated models as a function of the correlation coefficient between the original and predicted values, the degree to which these values rely on chance is reflected by the intercept with the y-axis. A model is generally considered valid if the intercept is negative for Q^2 and below 0.3 for R^2.[34]

References

1 V. Morell, *Science*, 1997, **278**, 575–576.
2 R. J. Williams and D. L. Heymann, *Science*, 1998, **279**, 1153–1154.
3 C. Walsh, *Nature*, 2000, **406**, 775–781.
4 D. Mirelman and I. Ofek, *Microbial Lectins and Agglutinins*, ed. D. Mirelman, Wiley, New York, 1986, p. 1–19.
5 K.-A. Karlsson, *Curr. Opin. Struct. Biol.*, 1995, **5**, 622–635.
6 H. Leffler and C. Svanborg-Edén, *FEMS Lett.*, 1980, **8**, 127–134.
7 G. Källenius, R. Möllby, S. B. Svensson, J. Winberg, A. Lundblad, S. Svensson and B. Cedergren, *FEMS Lett.*, 1980, **7**, 297–302.
8 K. Bock, M. E. Breimer, A. Brignole, G. C. Hansson, K.-A. Karlsson, G. Larsson, H. Leffler, B. E. Samuelsson, N. Strömberg, C. Svanborg-Edén and J. Thurin, *J. Biol. Chem.*, 1985, **260**, 8545–8551.
9 N. Strömberg, B.-I. Marklund, B. Lund, D. Ilver, A. Hamers, W. Gaastra, K.-A. Karlsson and S. Normark, *EMBO J.*, 1990, **9**, 2001–2010.
10 N. Strömberg, P.-G. Nyholm, I. Pascher and S. Normark, *Proc. Natl. Acad. Sci. U. S. A.*, 1991, **88**, 9340–9344.
11 I. M. Johansson, K. Plos, B.-I. Marklund and C. Svanborg, *Microb. Pathog.*, 1993, **15**, 121–129.
12 G. Otto, T. Sandberg, B.-I. Marklund, P. Ulleryd and C. Svanborg, *Clin. Infect. Dis.*, 1993, **17**, 448–456.
13 J. R. Johnson, T. A. Ruso, J. J. Brown and A. Stapleton, *J. Infect. Dis.*, 1998, **177**, 97–101.
14 M. Hedlund, M. Svensson, A. Nilsson, R. D. Duan and C. Svanborg, *J. Exp. Med.*, 1996, **1843**, 1037–1044.
15 M. Hedlund, C. Wachtler, E. Johansson, L. Hang, J. E. Somerville, R. P. Darveau and C. Svanborg, *Mol. Microbiol.*, 1999, **33**, 693–703.
16 S. Haataja, K. Tikkanen, U. Nilsson, G. Magnusson, K.-A. Karlsson and J. Finne, *J. Biol. Chem.*, 1994, **269**, 27466–27472.
17 R. Striker, U. Nilsson, A. Stonecipher, G. Magnusson and S. J. Hultgren, *Mol. Microbiol.*, 1995, **16**, 1021–1029.
18 J. Ohlsson, J. Jass, B. E. Uhlin, J. Kihlberg and U. J. Nilsson, *ChemBioChem*, 2002, **3**, 772–779.
19 K. W. Dodson, J. S. Pinkner, T. Rose, G. Magnusson, S. J. Hultgren and G. Waksman, *Cell*, 2001, **105**, 733–743.
20 (*a*) H. C. Hansen, S. Haataja, J. Finne and G. Magnusson, *J. Am. Chem. Soc.*, 1997, **119**, 6974–6979; (*b*) during the preparation of this paper dendritic galabiose compounds with low nanomolar affinity for *Streptococcus suis* adhesins were reported:J. A. F. Joosten, V. Loimaranta, C. C. M. Appeldoorn, S. Haataja, F. A. E. Maate, R. M. J. Liskamp, J. Finne and R. J. Pieters, *J. Med. Chem.*, 2004, **47**, 6499–6508.
21 A. Larsson, J. Ohlsson, K. W. Dodson, S. J. Hultgren, U. J. Nilsson and J. Kihlberg, *Bioorg. Med. Chem.*, 2003, **11**, 2255–2261.
22 J. Ohlsson and G. Magnusson, *Carbohydr. Res.*, 2000, **329**, 49–55.
23 E. D. Soli and P. DeShong, *J. Org. Chem.*, 1999, **64**, 9724–9726.
24 C. Peto, G. Batta, Z. Gyorgydeak and F. Sztariskai, *Liebigs Ann. Chem.*, 1991, 505–507.
25 P. Sörme, Y. Qian, P.-G. Nyholm, H. Leffler and U. J. Nilsson, *ChemBioChem*, 2002, **3**, 183–189.
26 P. Konradsson, U. E. Ududong and B. Fraser-Reid, *Tetrahedron Lett.*, 1990, **31**, 4313–4316.
27 G. H. Veeneman, S. H. van Leeuwen and J. H. van Boom, *Tetrahedron Lett.*, 1990, **31**, 1331–1334.
28 Scrubber 1.1f, 2000, BioLogic Software Pty Ltd, Unit 30 116 Blamey Crescent, Campell, ACT 2612, Australia.
29 J. Ohlsson, A. Sundin and U. J. Nilsson, *Chem. Commun.*, 2003, 384–385.
30 S. Haataja, K. Tikkanen, J. Liukkonen, C. François-Gerard and J. Finne, *J. Biol. Chem.*, 1993, **268**, 4311–4317.
31 MOE 2003.02, 2003, Chemical Computing Group Inc., 1010 Sherbrooke St. West Suite 910 Montreal, Canada H3A 2R7.
32 S. Wold, in *Chemometric methods in molecular design*, ed. H. van de Waterbeemd, Wiley, Weinheim, 1995, p. 195–218.
33 Simca-P 10.02′, 2002, Umetrics, Box 7960, S-907 19 Umeå, Sweden.
34 L. Eriksson, E. Johansson and S. Wold, in *Quantitative Structure-Activity Relationships in Environmental Sciences-VII*, ed. F. Chen and G. Schüürmann, 1997, SETAC Press, Pensacola, FL, p. 381–397.
35 J. Ohlsson and U. J. Nilsson, *Tetrahedron Lett.*, 2003, **44**, 2785–2787.